Scientific paper

The Ion-Storage Capacity and Surface Characterization of Ce/Cu Thin Films

Irena Kozjek Škofic,[a] Janez Kovač[b] and Nataša Bukovec[a]*

[a]*Faculty of Chemistry and Chemical Technology, University of Ljubljana, Aškerčeva 5, SI-1000 Ljubljana, Slovenia*

[b]*Jožef Stefan Institute, Jamova 39, SI-1000 Ljubljana, Slovenia*

** Corresponding author: E-mail: natasa.bukovec@fkkt.uni-lj.si*

Received: 02-04-2008

Dedicated to the memory of Professor Ljubo Golič

Abstract

Ce/Cu mixed oxide thin films with molar ratio 1 were prepared by sol-gel method and dip-coated on SnO_2/F covered glass. The cyclic voltammetry and chronocoulometry were carried out to determine their suitability for application as a counter-electrode in electrochromic devices. The charge capacity is up to 20 mC cm^{-2}, however, the reversibility of the redox process decreases with the number of cycles. Surface composition and chemical bonding of elements on the surface of the cycled and non-cycled part of the Ce/Cu mixed oxide thin film were investigated by X-Ray photoemission spectroscopy (XPS) and surface morphology was analyzed by atomic force microscopy (AFM). The Cu atoms on the non-cycled surface are bonded as Cu(2+), whereas after cycling the Cu atoms are reduced to Cu(1+). The Ce atoms in both areas are in the Ce(4+) state. The Ce/Cu ratio measured by XPS on the surface of the non-cycled area is higher than on the surface of the cycled one. In the cycled area the Li is present, bonded in thin film as Li_2CO_3.

Keywords: Ce/Cu mixed oxide thin film, counter-electrode, sol-gel process, XPS, AFM

1. Introduction

The ion-storage thin film materials should offer high charge capacity and high transparency in the visible region in both, reduced and oxidized states. Pure CeO_2 has been extensively studied in recent years as a candidate for optically passive counter-electrode in electrochromic devices. It exhibits a good reversibility of lithium intercalation, is highly transparent over the whole visible range, nevertheless its charge capacity is too low for the application in EC device. The limiting step is the diffusion of Li^+ ions into CeO_2.[1–4]

CeO_2 mixed with other oxides (TiO_2, ZrO_2, V_2O_5) have been prepared and investigated to improve the charge capacity of CeO_2 and to preserve its excellent transparency.[5–9] Several techniques, such as reactive DC magnetron sputtering, pulsed laser deposition, electron beam evaporation, spray pyrolysis and sol-gel methods have been applied in the synthesis of mixed thin films.[9–13] The sol-gel method has some advantages over others because a high degree of homogeneity of thin films can be achieved in a single or even in multicomponent systems. The electrochemical properties of these materials also depend on their preparation mode. The influence of annealing time and temperature on the structure of the thin films has already been reported.[9,14]

Several authors report that mixed oxides CeO_2–CuO have been proposed as potential candidates for CO catalysis. CeO_2–CuO oxides have been synthesized by a number of preparation modes, sol-gel method being one of them.[15,16] CeO_2 and copper do not form a solid solution because the cell unit of ceria is hardly affected by the presence of copper. Copper oxide acts as a bridging agent between the neighbouring CeO_2 crystallites and reduces their growth.[17]

The aim of our work was to investigate whether CeO_2–CuO thin films can be used as a counter-electrode in electrochromic device. In this paper, we report on preliminary results of a research work based on mixed CeO_2–CuO coatings prepared by sol-gel technique. TG analysis was used to determine the annealing temperature

of thin films. XPS (X-Ray photoelectron spectroscopy) and AFM (Atomic force microscopy) analysis of this sample before and after lithium intercalation was performed and some preliminary electrochemical characterization has been presented.

2. Experimental

Sols of Ce/Cu mixed oxide films were prepared by dissolving $CeCl_3 \cdot 7H_2O$ and $Cu(CH_3COO)_2 \cdot H_2O$ with a molar ratio 1 in a mixture of citric acid and ethanol according to literature.[9] The dark green clear sols obtained were stable for a few weeks at room temperature. Thin films were deposited by dip-coating technique on a transparent glass with a conductive coating of fluorine-doped thin dioxide (SnO_2/F, Pilkington, K-glass, $R_{\square}$=13 Ω $\square^{-1}$). The glass plates were previously cleaned with ethanol and distilled water using an ultrasonic cleaner for 5 min and dried before depositing. After pulling the films were dried in air at room temperature followed by heat-treatment for 20 min.

For thermoanalytical measurements thin films were deposited on Al foil, cut with scissors into smaller pieces. Thermogravimetric (TG) measurements (dynamic and isothermal) were performed in air atmosphere with a flow rate 100 mL/min using a Mettler Toledo TA/SDTA 851^e thermoanalyser in temperature range of 25 to 500 °C. The heating rate was 5 K/min. Isothermal measurements were performed in two steps: the furnace was heated at 5 K/min to a chosen temperature (350, 400, 450 °C), left for an hour then heated up to 500 °C and left for 30 min at that temperature. Platinum crucibles were used. The base line was subtracted in all cases. Differential scanning calorimetry (DSC) of the samples was performed on a Metller Tolledo DSC 822^e at the heating rate 5 K/min and aluminium crucibles were used.

X-Ray diffraction (XRD) was measured using a PANalytical X'Pert PRO MPD diffractometer with $CuK_{\acute{a}}$ radiation from 10 to 70 with a step of 0.025° 2Ω per second.

Electrochemical measurements were performed using an EG&G PAR273 computer-controlled potentiostat-galvanostat consisting of a three electrode cell, filled with 1 M $LiClO_4$ in propylene carbonate (PC). The working electrode was a Ce/Cu mixed oxide thin film deposited on SnO_2/F coated glass with a surface area 1 cm^2. The reference electrode was Ag/AgCl filled with a mixture of 1 M LiCl in methanol and 1 M $LiClO_4$ in PC with a molar ratio 1:9, platinum electrode serving as counter-electrode. Cyclic voltammetry (CV) was performed at potentials between +1.6 and –1.6 V with a scanning rate of 50 mV/s and chronocoulometric (CPC) measurements at potentials –1.6 and +1.6 V for 100 s.

The X-Ray photoelectron spectroscopy (XPS or ESCA) analyses were carried out on the PHI-TFA XPS spectrometer produced by Physical Electronics Inc. The analysed area was 0.4 mm in diameter and the analysed depth was about 1–3 nm. This high surface sensitivity is a general characteristic of the XPS method. Sample surfaces were excited by X-Ray radiation from the Al source with photon energy of 1486.6 eV. The wide-scan survey spectra were acquired with an analyser pass energy of 187 eV. The narrow-scan spectra of C 1s, O 1s, Cu 2p, Ce 3d, Sn 3d, Li 1s were obtained with an analyser pass energy of 58 eV, yielding energy resolution of about 1.0 eV. During data processing the spectra from the surface were aligned by setting the C 1s peak at 284.8 eV. The accuracy of binding energies was about 0.3 eV. Quantification of surface composition was performed from XPS peak intensities taking into account relative sensitivity factors provided by instrument manufacturer.[18] The relative error of the concentration calculated is estimated to be 20 %. The measurement of surface morphology was performed by AFM microscope model Solver Pro, produced by NT-MDT company. The topographic images of surface were acquired in a semi-contact mode over ranges from 500 x 500 nm^2 to 20 x 20 μm^2 by the Si tips with a force constant of 10 N/m.

3. Results and Discussion

Figure 1 presents dynamic TG and DSC curves of Ce/Cu thin films. The decomposition reactions in thin film samples take place simultaneously. The first mass loss in the temperature range from 25 to 130 °C is ascribed to the evaporation of ethanol and water. On the DSC curve endothermic peak is positioned at 108 °C. The second step in the weight loss curve from 130 to 270 °C is connected with thermal decomposition of citric acid, which is showed on the DSC curve as a broad exothermic peak, centred at 213 °C. The third step, from 270 to 500 °C, is associated with several structural changes which are not connected with a considerable mass loss.

In our previous studies we found that the charge capacity depends on thermal treatment: too high annealing

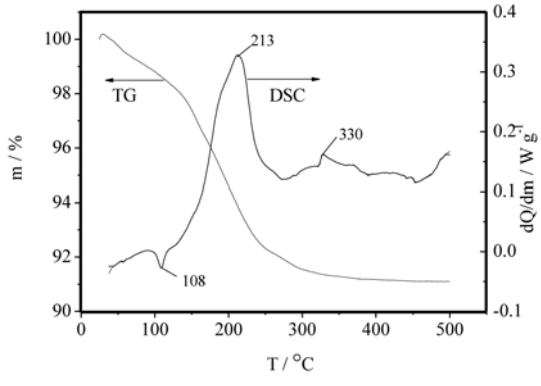

Figure 1. TG and DSC curve of Ce/Cu mixed oxide thin film.

temperature leads to poor reversibility of the ion-storage process of the film.[18] For these reason we performed some isothermal TG measurements at 350, 400, 450 and 500 °C.

The isothermal TG curves show that final weight loss was not achieved by the samples heated at 350 °C for an hour (Figure 2). Thin films prepared at 350 °C (and also with a short annealing time 20 min) had low charge capacity and poor reversibility of the ion-storage process (Table 1). Prolongation of the annealing time (60 min) only slightly improved the ion-storage capacity of the film. Thin films, heat-treated at 400 °C for 20 or 60 min, had appropriate electrochemical properties. The charge capacity increased during first 50 cycles, then remained stable for another 200 cycles. If the annealing time was prolonged (60 min), the charge capacity was slightly decreased, but the values of inserted charge were still up to 20 mC cm^{-2}. Heat-treatment of thin film at 450 °C increased grain size in the film and consequently the charge capacity decreased. The charge capacity of the thin film annealing at 500 °C was so low that we made no further investigations.

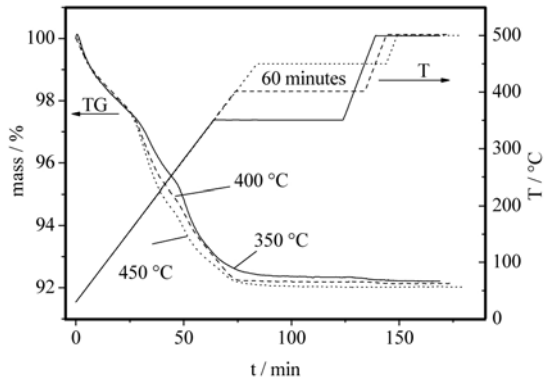

Figure 2. Isothermal TG curves of Ce/Cu thin films at 350 (__), 400 (_) and 450 °C (...). The heating rate was 5 K/min.

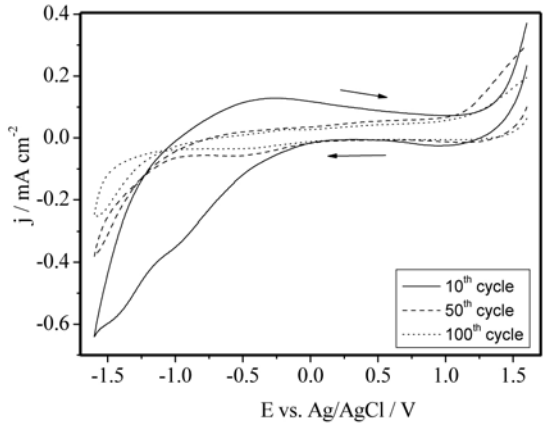

Figure 3. Cyclic voltammograms of Ce/Cu mixed oxide thin film heat-treated for 20 min at 400 °C. The scan rate was 50 m V/s.

Cyclic voltammograms (CV) of mixed oxide of Ce/Cu thin film are presented in Figure 3. A major change in the discharge behaviour occurred between the 10th and the 50th cycle where large variations in current density were observed.

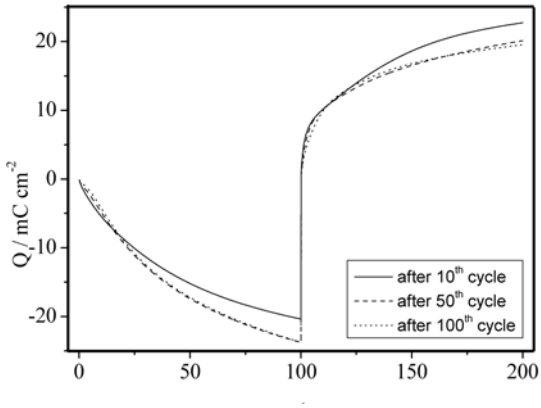

Figure 4. Chronocoulometric curves of Ce/Cu mixed oxide thin film at potentials –1.6 V and +1.6 V. Measurement time: 100 s.

Table 1. Chronocoulometric measurements of Ce/Cu thin films annealed for 20 min at 350, 400 and 450 °C with the corresponding intercalated (Q_i) and extracted (Q_e) charges.

T/ °C	t/min	1st cycle Q_i/Q_e mC cm^{-2}	10th cycle Q_i/Q_e mC cm^{-2}	50th cycle Q_i/Q_e mC cm^{-2}	100th cycle Q_i/Q_e mC cm^{-2}
350	20	–6.8/4.4 (0.65)	–5.8/3.8 (0.66)	–6.5/4.1 (0.63)	–7.5/4.9 (0.65)
	60	–7.2/5.0 (0.69)	–6.8/5.6 (0.82)	–7.7/5.6 (0.73)	–8.5/6.0 (0.71)
400	20	–19.8/19.3 (0.97)	–20.4/22.7 (1.11)	–23.8/20.1 (0.84)	–23.7/19.5 (0.82)
	60	–19.2/13.4 (0.70)	–18.9/17.3 (0.92)	–21.4/18.2 (0.85)	–21.9/17.2 (0.79)
450	20	–10.0/9.1 (0.91)	–11.3/11.6 (1.03)	–17.9/18.9 (1.06)	–17.8/19.3 (1.08)
	60	–4.4/3.2 (0.73)	–4.4/3.9 (0.87)	–4.9/4.4 (0.90)	–5.7/4.9 (0.86)

Figure 4 illustrates the cycling dependence of the inserted and extracted charge densities. After the first cycle the intercalation/deintercalation of Li ions increased up to the 50th cycle and afterwards remained stable. The kinetic rates of the insertion and deinsertion of Li ions are similar as can be seen from Figure 4.

During cycling the colour of the thin film changed colour from brownish yellow to yellow. The XRD analysis of the Ce/Cu thin film with less than 100 nm thickness resulted only in SnO_2 peaks which were associated with the substrate glass. The XRD analysis of xerogels showed that the crystallites of CeO_2 were very small, while the peaks of CuO could not be observed.

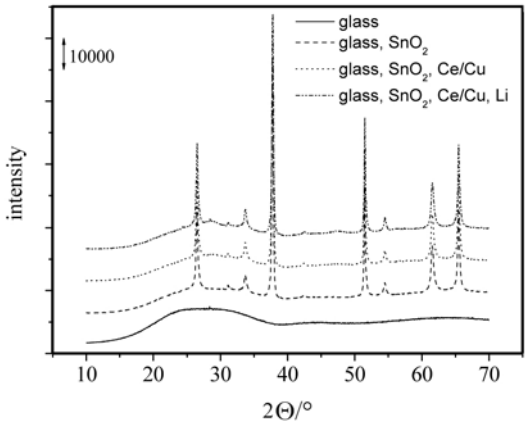

Figure 5. XRD spectra of thin films (glass (—), glass with SnO_2 (_), glass with SnO_2 and Ce/Cu (...), cycled Ce/Cu on SnO_2 covered glass in $LiClO_4$/PC (. . .)).

For better comparison XPS and AFM analyses were performed on the same thin film. Half of the Ce/Cu thin film, heat-treated at 400 °C for 20 min, was immersed into electrolyte and cycled. Figure 6 shows the morphology of Ce/Cu mixed oxide thin film on the non-cycled and cycled areas of the same thin film on the scale of 500 nm. The cycled layer consists of round-shaped grains of average dimension of 50–70 nm in diameter. The grains in the cycled area are smaller. We estimated that their size is 20–50 nm in diameter.

Figure 7 shows surface morphology on both areas at a larger scale (20 μm). On this scale the surface of the non-cycled thin film is homogenous and flat and covered uniformly by grains which prove that Ce/Cu mixed oxide thin film is compact. The layer on the cycled thin film shows substantially different morphology. The layer is partially removed and damaged. It is evident that cycling causes the reduction of the grain size and partially removes the Ce/Cu mixed oxide thin film.

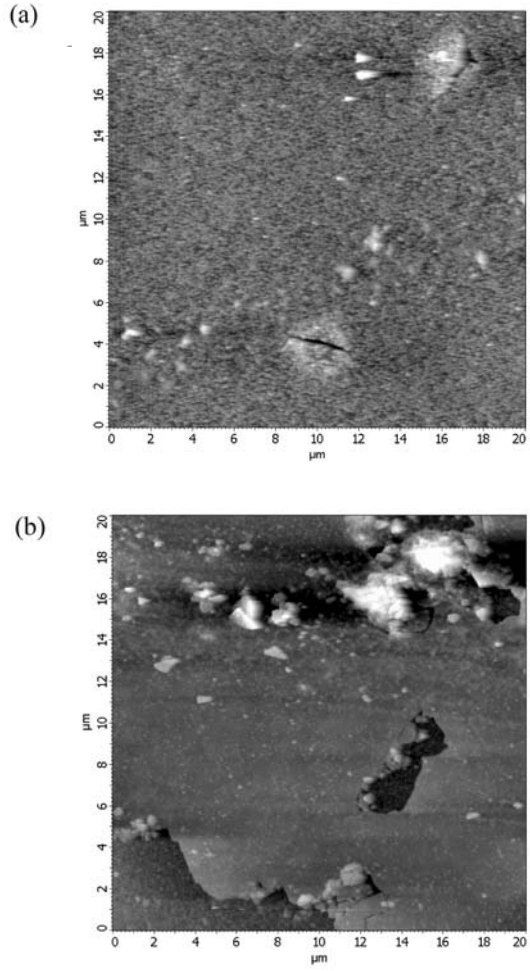

Figure 7. AFM images of the non-cycled (a) and cycled (b) area of the Ce/Cu mixed oxide thin film on the 20 x 20 μm scale.

Figure 8 shows XPS survey spectra from both areas. Characteristic peaks of C 1s, O 1s, Cu 2p and Ce 3d are present in the spectrum of the non-cycled thin film. In ad-

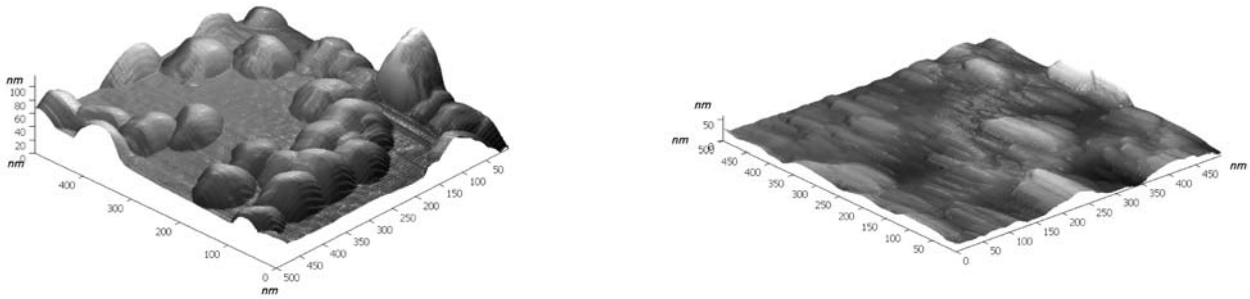

Figure 6. AFM images of non-cycled (a) and cycled (b) areas of the Ce/Cu mixed oxide thin film in 1 M $LiClO_4$/PC.

Table 2. Surface composition in mol.% of the non-cycled (a) and cycled (b) areas of the Ce/Cu mixed oxide thin film derived by XPS method.

Sample	O	C	Cu	Ce	Sn	Li
a	43.5	29	18.8	8.2	0.5	0
b	48.3	22.7	4.7	3.3	4.5	16.5

dition the XPS spectrum from the cycled thin film also contains Sn 3d and Li 1s peaks. Surface composition was calculated from the intensities of elemental peaks in the XPS spectra and the results are presented in Table 2 and in the bar graph (Figure 9).

On the surfaces of both areas, C and O are the most abundant elements. The part of carbon may originate from the film deposition process. This can be ascribed to surface contamination due to exposure to the air, thermal decomposition of citric acid, or is a residue of electrolyte solution. Elements Cu, Ce and O are related to the thin film oxide layer. The Ce/Cu ratio in the cycled thin film is higher (0.70) than in the non-cycled one (0.44), and the Ce and Cu are present on the non-cycled thin film to a greater extent than in the cycled area. The latter can be explained by partial removal of the Ce/Cu mixed oxide thin film during the cycling, as it was evidenced above by surface morphology change shown in the AFM images.

Partial removal of the Ce/Cu mixed oxide thin film is proved also by much higher concentration of Sn, originating from the Sn-sublayer, since after cycling this layer is not completely covered. Further insight into the Ce/Cu mixed oxide thin film can be obtained by the analysis of peak shapes and binding energies of the XPS peaks. XPS method does not only provide the information on surface composition but it is also a sensitive tool for identifying

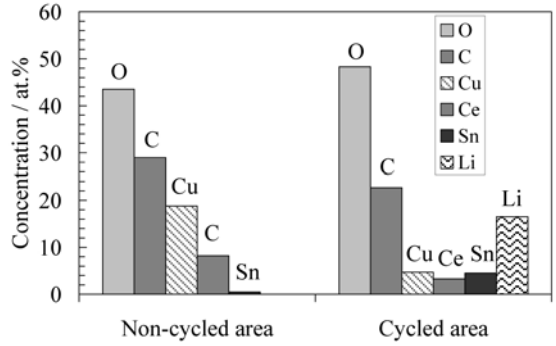

Figure 9. Surface composition of the non-cycled and cycled areas of the Ce/Cu mixed oxide thin film obtained by XPS method.

the chemical state of elements on the surface. Figure 10 shows the Cu 2p and Ce 3d peaks in the binding energy region between 870 and 970 eV. The main Ce 3d peak on both areas are at the binding energy of 882 eV, which is characteristic for Ce(4+) ions.[19] The absence of Ce 3d peak at the energy of 905 eV, which is characteristic for Ce(3+) ions, meaning that the Ce atoms are bonded in only one chemical state Ce(4+) on both areas. A closer analysis of the Cu 2p peaks shows that the main peak Cu $2p_{3/2}$ is at 933 eV. This peak may correspond to Cu in different chemical states (Cu-metallic, Cu(1+) and Cu(2+)), therefore it can not be used for chemical state identification. But the additional peak at 942–944 eV (the so called shake-up plasmon) is characteristic only for Cu(2+) ions. This peak is present in the Cu 2p spectrum and its intensity from the non-cycled area means that the Cu atoms are present in Cu(2+) ions, whereas in the cycled area the Cu atoms are mainly in Cu(1+), and to a lesser extent also in Cu(2+). Another feature found in the cycled thin film is

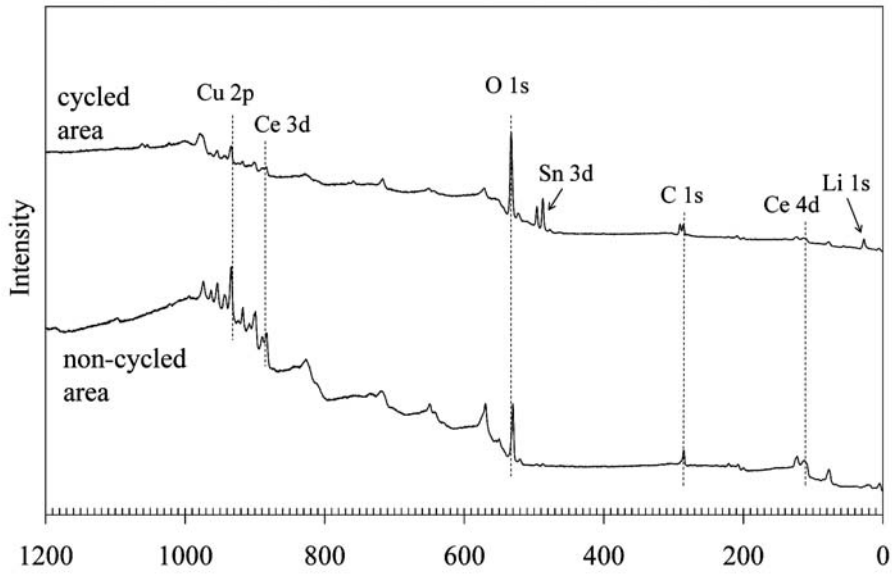

Figure 8. XPS survey spectra from non-cycled and cycled areas of the Ce/Cu oxide layer.

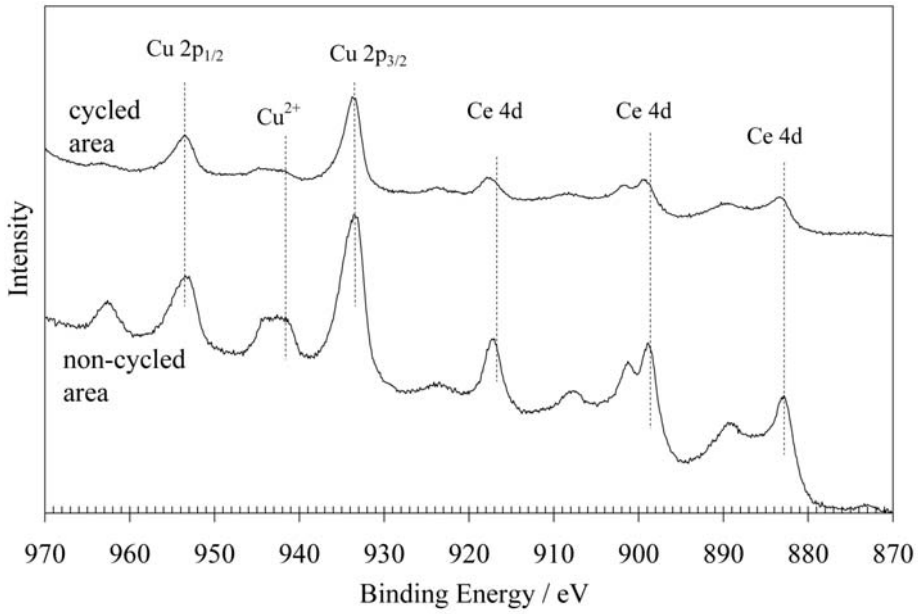

Figure 10. XPS spectra of Cu 2p and Ce 3d from non-cycled and cycled areas of the Ce/Cu mixed oxide thin film.

the presence of Li. This shows that Li atoms have been incorporated into the Ce/Cu mixed oxide thin film during sample cycling. Binding energies of Li 1s peak at 55.4 eV and C 1s peak at 290.2 eV (not shown) indicate the presence of thin Li_2CO_3 thin film on the cycled area of the sample.[19]

4. Conclusions

Ce/Cu mixed oxide thin films were prepared by sol-gel process using $CeCl_3 \cdot 7H_2O$ and $Cu(CH_3COO)_2 \cdot H_2O$ as precursors. The electrochemical characteristics of thin film depended on the annealing temperature and time. The films annealed at 400 °C for 15 min had better electrochemical characteristics than the films annealed at 350 and 450 °C. Prolongation of the annealing time decreased ion-storage capacity of the thin film. Morphology difference between non-cycled and cycled areas of the Ce/Cu mixed oxide thin film showed that during cycling the Ce/Cu mixed oxide grains became smaller and that this layer was partially removed and damaged. During the cycling lithium was incorporated into the Ce/Cu mixed oxide thin film. Chemical state of Ce(4+) was identified in both areas, however during cycling Cu(2+) ions were mainly changed to Cu(1+) on cycled area of the thin film.

5. Acknowledgements

The authors gratefully acknowledge the Ministry of Aducation, Science and Sport of Republic of Slovenia for the financial support of the present study within the research program P1-0134-0103. The authors would also like to thank Tatjana Filipič for her help with XPS and AFM measurements and prof. dr. Anton Zalar for helpful discussions.

6. References

1. N. Özer, *Sol. Energy Mater. Sol.* Cells **2001**, *68,* 391–400.
2. I. Kozjek Škofic, S. Šturm, M. Čeh, N. Bukovec, *Thin Solid Films* **2002**, *422,* 170–175.
3. I. Porqueras, C. Person, C. Corbella, M. Vives, A. Pinyol, E. Bertran, *Solid State Ionics* **2003**, *165,* 131–137.
4. A. Siokou, S. Ntais, V. Dracopoulos, S. Papaefthimiou, G. Leftheriotis, P. Yianoulis, *Thin Solid Films* **2006**, *514*, 87–96.
5. U. Lavrenčič Štangar, B. Orel, I. Grabec, B. Ogorevc, K. Kalcher, *Sol. Energy Mater. Sol. Cells* **1993**, *31*(2), 171–185.
6. A. Verma, A.G. Joshi, A.K. Bakhshi, S.M. Shivaprasad, S.A. Agnihotry, *Appl. Surf. Sci.* **2006**, *252,* 5131–5142.
7. C. O. Avellaneda, L. O. S. Bulhões, A. Pawlicka, *Thin Solid Films* **2004**, 471, 100–104.
8. U. Opara Krašovec, B. Orel, A. Šurca, N. Bukovec, R. Reisfeld, *Solid State Ionics* **1999**, *118,* 195–214.
9. I. Kozjek Škofic, N. Bukovec, *Acta Chim. Slov.* **2002**, *49*, 267–278.
10. A. Azens, L. Kullman, D.D. Ragan, C.G. Granqvist, Sol. Energy *Mater. Sol. Cells* **1998**, *54,* 85–91.
11. J. Horwitz, J. Spragie, in: D.B. Chrisey, G.K. Hubler (Eds.), *Pulsed Laser Depositin of Thin Films,* John Wiley & Sons, New York, **1994**, pp 229.

12. G. Atanasov, R. Thielsch, D. Popov, *Thin Solid Films* **1993**, *223*(2), 288–292.
13. B. Elidrissi, M. Addou, M. Regragui, C. Monty, A. Bougrine, A. Kachouane, *Thin Solid Films* **2000**, *379*, 23–27.
14. R. Cerc Korošec, P. Bukovec, B. Pihlar, J. Padežnik Gomilšek, *Thermochim. Acta* **2003**, *402,* 57–67.
15. S. Hočevar, U. Opara Krašovec, B. Orel, A.S. Aricó, H. Kim, *Appl. Catal.* B **2000**, *28,* 133–125.
16. X. Wu, Q. Liang, D. Weng, Z. Lu, *Catal. Com.* **2007,** *8*(12), 2110–2114.
17. G. Marbán, A.B. Fuertes, *Appl. Catal.* B **2005**, *57*, 43–53.
18. J. F. Moulder, W. F. Stickle, P. E. Sobol, K. D. Bomben, Handbook of X-Ray Photoelectron Spectroscopy, Physical Electronics Inc., Eden Prairie, Minnesota, USA, **1995**.
19. Andersson, A. Henningson, H. Siegbahn, U. Jansson, K. Edström, *J. Power Sources* **2003**, 119–212, 522–527.

Povzetek

Tanke plasti mešanega oksida Ce/Cu z množinskim razmerjem 1 smo pripravili po sol-gel postopku in s tehniko potapljanja nanesli na z SnO_2/F prevlečeno steklo. Za določanje ustreznosti pripravljene tanke plasti za uporabo v elektrokromnem sklopu smo uporabili ciklično voltametrijo in kronokoulometrijo. Velikost interkaliranega naboja je nad 20 m-C cm^{-2}, reverzibilnost redoks procesov se s številom ciklov zmanjšuje. Strukturne in kemijske spemembe na površini tanke plasti, ki so nastale med ciklanjem, smo preučevali z XPS in AFM. Baker je v neciklani tanki plasti v obliki Cu(2+), med ciklanjem se v večji meri reducira do Cu(1+). Cerij je v ciklani in neciklani tanki plasti v obliki Ce(4+). Množinsko razmerje med cerijem in bakrom, merjeno z XPS, se na površini tanke plasti med ciklanjem spreminja in je pri neciklanem filmu večje kot pri ciklanem. V ciklani tanki plasti smo določili prisotnost litija, ki je v obliki Li_2CO_3.